High Efficiency Semiconductor-Liquid Junction Solar Cells based on Cu/Cu_2O

Fang Shao, Jing Sun, Lian Gao, Jianqiang Luo, Yangqiao Liu, and Songwang Yang*

Cu/Cu_2O photoelectrodes are synthesized by a simple electrodepositing process at low temperature. The values of the electrolyte pH have great influence on the morphology and the compositions of the obtained films, and thus affect the performance of the electrodes. The best device based on Cu/Cu_2O and I^-/I_3^- electrolyte gives a high conversion efficiency of 3.13% under simulated AM1.5G illumination. To the best of our knowledge, this is the highest efficiency reported for solar cells based on electrodeposited Cu_2O. For comparison purposes, pure Cu_2O films are also synthesized. The performance of the solar cells based on pure Cu_2O is very poor, as low as 0.013%. In addition, the Cu/Cu_2O films are perfectly compatible with the lightweight plastic substrates and yielded a power conversion efficiency of 1.44%.

1. Introduction

In view of the severe ecological impacts of fossil fuels, solar energy has been extensively investigated as the cleanest and least limited energy source. The development of solar energy converters with good performance and low cost requires the availability of inexpensive, non-toxic materials with potential application in solar energy converting.

Cuprous oxide (Cu_2O) is an interesting p-type semiconductor with a band gap of 2 eV, which makes it suitable for solar cell applications.[1–6] The theoretical energy conversion efficiency of Cu_2O is 20%.[7,8] What's more, Cu_2O is a non-toxic and cheap material.[9] Owing to the solar light absorption of Cu_2O, Cu_2O/TiO_2 has already exhibited enhanced performance as catalysts compared with TiO_2.[10–13] Many Cu_2O based solar cells have also been reported, however, the preparation process is time and energy consuming or the efficiencies are very low.[14–17] The highest efficiency ever reported for any Cu_2O based solar cell is 2%.[18] The majority of absorption occurs in the Cu_2O; photogenerated carriers are transported through the Cu_2O to a collection electrode. The Cu_2O was prepared by oxidizing copper at a high temperature, which is so far the most popular method for the production of Cu_2O used in solar cells. The quality of the Cu_2O synthesized by this method is relatively good. But during the oxidation, the temperature is above 1000 °C and the O_2 partial pressure should be controlled. So this method has more requirements on equipments, and is more energy consuming. In contrast, electrodeposition is simple, scalable and inexpensive, which requires minimal energy input.[19] However, the electrodeposited Cu_2O films have a high resistivity and thus the solar cells based on electrodeposited Cu_2O often offer a poor performance. For example, hetero-junctions of Cu_2O/ZnO have been synthesized and used in solar cells, yielding an efficiency of 0.47%.[19] Chen et al.[20] reported the deposition of Cu_2O onto vertical ZnO nanowires. The fabricated Cu_2O/ZnO solar cell exhibited an over all conversion efficiency of around 0.1%.

Using electrodeposition method, both pure Cu_2O and Cu/Cu_2O can be easily obtained. In the conventional solid-state photovoltaic devices, Cu metal is deleterious. It lowers the barrier heights of the Schottky junctions and limits the open-circuit voltage to below 350 mV. So many efforts have been made to minimize the Cu formation. However, Cu has good electric conductivity, which may be beneficial to charge collecting and transferring.[21] In addition, the transmission light could be reflected by Cu metal and recycled, which would enhance the light harvesting ability. The dominant photovoltaic mechanisms in $Cu\text{-}Cu_2O$ junctions are electron injection from Cu_2O into Cu when $h\nu > E_g$ and hole photoemission from Cu into Cu_2O when $h\nu < E_g$.[22,23]

Semiconductor-liquid junction solar cells have attracted more and more concern in recent years.[24–26] Semiconductor-liquid junctions offer the opportunity to fabricating a more efficient solar cell based on Cu_2O. In aqueous solutions, Cu_2O is usually not stable while in acetonitrile or other nonaqueous electrolytes, Cu_2O exhibits a more stable property.[27,28] Lewis et al.[27] prepared nonaqueous liquid junction solar cells with Cu_2O photoelectrodes and resulted in an efficiency of 1.5%.

In this paper, Cu/Cu_2O and pure Cu_2O films were synthesized by electrodepositon from solutions at low temperature. The materials are abundant, cheap, and non-toxic, the fabrication method is simple and cheap, which is suitable for industrial production. The pH values of the electrolyte have great influence on the morphology and the compositions of the obtained films, and thus affect the performance of the cells. The best solar cell which is based on Cu/Cu_2O films, reached an open-circuit voltage of 0.56 V, a short-circuit current density of

F. Shao, Prof. J. Sun, Prof. L. Gao, Dr. J. Luo, Prof. Y. Liu, Dr. S. Yang
The State Key Lab of High Performance Ceramics and Superfine Microstructure
Shanghai Institute of Ceramics
Chinese Academy of Sciences
Shanghai 200050, P. R. China
E-mail: jingsun@mail.sic.ac.cn

DOI: 10.1002/adfm.201200365

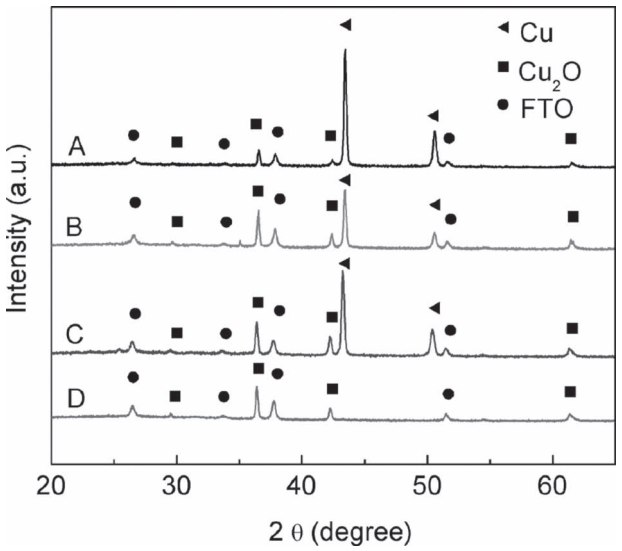

Figure 1. XRD patterns of the films on FTO glasses deposited with different pH and time (min). (A) Cu/Cu_2O-5.0-20, (B) Cu/Cu_2O-5.4-20, (C) Cu/Cu_2O-5.4-60, (D) Cu_2O-5.8-20.

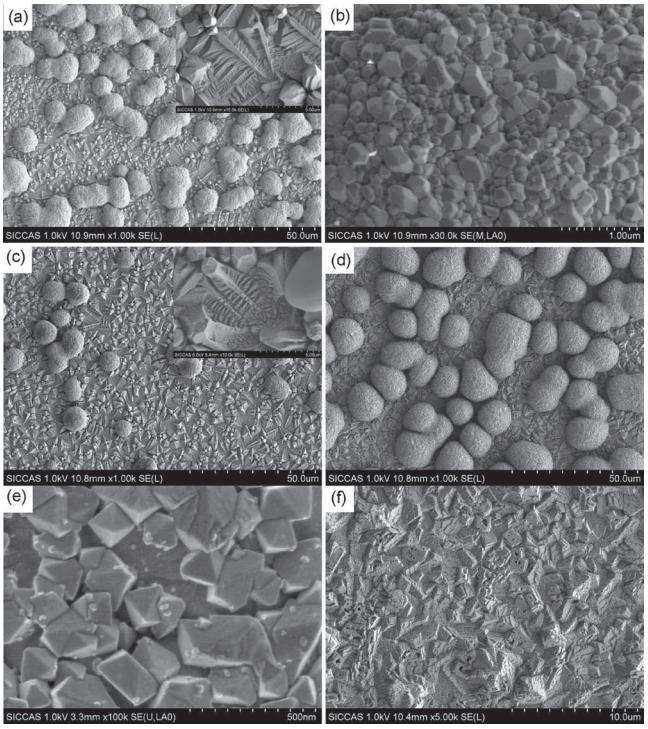

Figure 2. SEM images of (a) Cu/Cu_2O-5.0-20, (b) the surface of spheres in Cu/Cu_2O-5.0-20, (c) Cu/Cu_2O-5.4-20, (d) Cu/Cu_2O-5.4-60, (e) the spheres' surface of Cu/Cu_2O-5.4-60, (f) Cu_2O-5.8-20. The inset images in (a,c) shows the corresponding morphology at higher resolution. The scale bars of the insets are both 5 μm.

11.3 mA/cm^2, a fill factor of 49.6%, and a conversion efficiency of 3.13% under simulated AM1.5G illumination. To the best of our knowledge, this is the highest efficiency value reported for solar cells based on electrodeposited Cu_2O.

2. Results and Discussion

The electrodeposition of Cu_2O includes two steps, one is the cathodic reduction of Cu^{2+} ions to Cu^+ ions and the other is the deposition of Cu_2O due to the solubility limitation of Cu^+ ions.[29] This reaction is $2Cu^{2+} + 2e^- + H_2O \rightarrow Cu_2O + 2H^+$. There was another reaction during the reduction of cupric acetate: $Cu^{2+} + 2e^- \rightarrow Cu$. The electrolyte pH significantly dropped after the reaction due to the accumulation of H^+ ions. The experimental conditions involving pH and electrodeposition time have enormous influences on the composition and mophology of samples.

XRD patterns of the samples synthesized with different growth parameters are shown in **Figure 1**. The samples were denoted as Cu/Cu_2O-x-y or Cu_2O-x-y, where x (5.0, 5.4, or 5.8), y (20 or 60) referred to the corresponding pH and deposition time (min), respectively. When the pH is ~5.0 and ~5.4, the deposited films are all a composite of Cu and Cu_2O, while the films deposited at pH ~5.8 are pure Cu_2O. No peaks from CuO are present in these patterns. The results are consistent with previous reports.[2,29] It's worth noting that the intensity of Cu peaks increased with the increase of deposition time or the decrease of pH. It indicates that the contents of Cu metal in Cu/Cu_2O-5.0-20 and Cu/Cu_2O-5.4-60 are both higher than Cu/Cu_2O-5.4-20.

Furthermore, morphologies of the samples were examined by SEM (**Figure 2**). Figures 2a to e show the SEM images of Cu/Cu_2O-x-y while Figure 2f exhibits Cu_2O-5.8-20. We can see that there exist many differences between the two kinds of samples. Cu_2O-5.8-20 formed quasi-cuboid structure, while the Cu_2O crystal of Cu/Cu_2O-x-y took on a dendritic growth. This dendritic structure formed a physically continuous crystal body, which may be beneficial to charge-transport property. As shown in Figure 2a and c (the insets are the high magnified images), the dendritic crystals may be developed from polyhedral crystals due to the acetate ions preferentially adsorbed.[30] Besides, some spheres appeared in this kind of sample. In the cases of Cu/Cu_2O-5.0-20 and Cu/Cu_2O-5.4-20, the diameters of the spheres are in the range of 5–10 μm and the surfaces of the spheres are closely coated by a crystal layer (as shown in Figure 2b and Figure S1). The amounts of spheres in Cu/Cu_2O-5.0-20 are much more than those in Cu/Cu_2O-5.4-20. EDS results indicate that Cu and O are the only elementary components in these spheres, and their concentrations are 88.8 and 11.2 atom% in Cu/Cu_2O-5.0-20; 85.6 and 14.4 atom% in Cu/Cu_2O-5.4-20, respectively (Figure S2 and Figure S3). Figure 2d is the SEM image of Cu/Cu_2O-5.4-60, from which it can be seen that the spheres became more and larger with the prolongation of treating time. The crystals on the surfaces of the spheres exhibited the octahedral morphology (Figure 2e).

Figure 3 exhibits TEM images of a sphere in Cu/Cu_2O-5.4-60, it can be seen that there is a layer of nanocrystal at the outer part of the sphere except the bottom. Additional SEM and EDS characterizations were performed to study the structure of the films. We choose three characteristic points, as shown in Figure S4. Point 1 is a polyhedral crystal while point 2 is a large sphere,

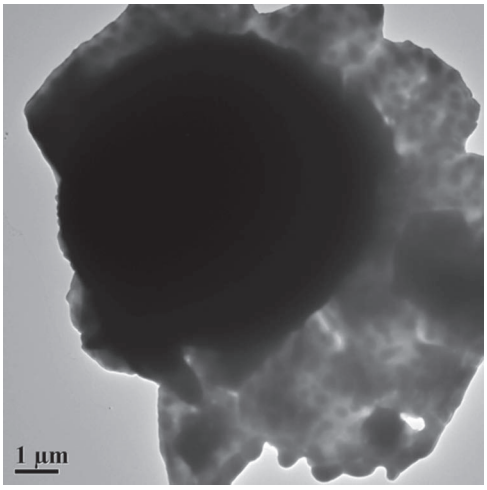

Figure 3. TEM image of a sphere of Cu/Cu_2O-5.4-60.

point 3 is the dendritic structure. The three selected parts can basically represent all the structures in the film. It has been generally accepted that the penetration depth of electron beam increase along with the accelerating voltage (Monte Carlo simulation). When the voltage was 3 KV and 5 KV, the Cu/O atomic ratios of the three points were all about 2:1, indicating the existence of pure Cu_2O (Table S1). At 8 KV, the compositions in point 1 and 2 had no obvious change while the electron beam went through point 3, giving information on FTO substrate (the fluorine-doped SnO_2 conducting glass). When the voltage increased to 15 KV, the contents of Cu at point 2 increased sharply, demonstrating that the core of the sphere is Cu. Cu concentrations continue to increase for point 2 at 20 KV, and Sn elements from FTO had been detected, indicating the direct connection of Cu with FTO at point 2. At that moment, point 1 was also penetrated. There were no increase of Cu at point 1 and 3 until penetrated, which suggests that the component of the structures between the spheres are pure Cu_2O.

In the case of Cu_2O-5.8-20, the growth process of the Cu_2O crystals deposited directly on the FTO substrate is favorable. However, when pH reduces and Cu is presents, Cu_2O crystals were frequently deposited on top of the exposed Cu, which provides nucleation sites for Cu_2O crystals.[31] The dense Cu_2O crystal layer could protect Cu by isolating Cu surface from the redox electrolytes.

The reflectance measurement could help to quantify the surface fraction occupied by the Cu/Cu_2O spheres. **Figure 4**a indicated that the Cu/Cu_2O spheres in Cu/Cu_2O-5.0-20 and Cu/Cu_2O-5.4-60 are much more prevalent than in Cu/Cu_2O-5.4-20 and Cu_2O-5.8-20, which is in good agreement with previous results. As shown in Figure 4b, the high Cu content results in greater loss of transmission. Compared with that of Cu_2O-5.8-20, the absorptance of Cu/Cu_2O-5.4-20 increased in a degree, while absorptance of Cu/Cu_2O-5.0-20 and Cu/Cu_2O-5.4-60 decreased to a certain extent. It is presumed that the incident light could be reflected by Cu/Cu_2O spheres and recycled, which would enhance the light harvesting ability in a degree. However, too much Cu results in less effective light. Though the differences are not enormous, these could also explain the

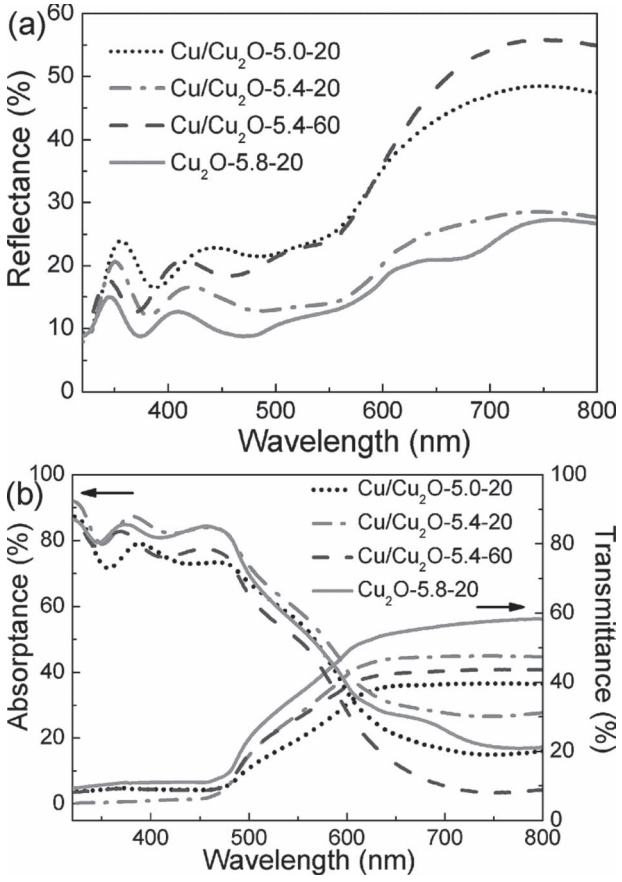

Figure 4. (a) Reflectance spectra, (b) transmittance and absorptance (1-transmittance-reflectance) spectra of the as-prepared samples (Cu/Cu_2O-5.0-20, Cu/Cu_2O-5.4-20, Cu/Cu_2O-5.4-60 and Cu_2O-5.8-20)

performance change of the various cells from light utilization side.

Sandwich type solar cells were constructed with the as-prepared samples and their performances were evaluated by recording the current density–voltage (J–V) curves under normalized illumination and dark condition. The characteristics are presented in **Figure 5** and the parameters for the cells prepared from four different photoanodes are reported in **Table 1**. When pure Cu_2O was used as the photoanode, the J–V curves of the cell took on a diagonal appearance. The short circuit current density (J_{SC}) and open-circuit voltage (V_{OC}) are both very low, which are 0.5 mA/cm^2 and 0.10 V, respectively. The fill factor (FF) is 25.3% and the efficiency (η) is 0.013%. The resistances of the pure Cu_2O films are above 10^6 Ω/□, resulting in a high series resistance of the corresponding cells and thus lead to the strong loss of photovoltaic efficiency. In any solar cell, there are parasitic resistances that will cause the limited performances. They can be divided into two parts, the series resistance (R_S) and the shunt resistance (R_{SH}). The resistance through the semiconductors is a big part of R_S, while the resistance of alternate electrical pathways that do not contribute to the photocurrent makes R_{SH}. In an ideal solar cell, R_S is zero, and R_{SH} is infinite.[32]

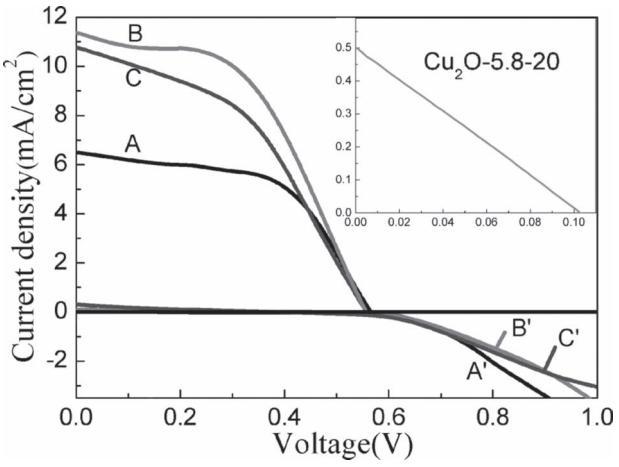

Figure 5. Current density-voltage characteristics measured under AM 1.5G at 100 mW cm^{-2} illumination for Cu/Cu_2O-5.0-20 (A), Cu/Cu_2O-5.4-20 (B) and Cu/Cu_2O-5.4-60 (C) based cells; (A′,B′,C′), corresponding currents in the dark for (A,B,C); the curve in the inside image is photocurrent-voltage plot of the cell based on Cu_2O-5.8-20.

For the solar cell based on Cu_2O-5.8-20, the R_S is 1695 Ω and R_{SH} is 1547 Ω. The results are consistent with the analyses above. On the other hand, when there is Cu in the solar cells, the whole performance increases sharply. As shown, the cell based on Cu/Cu_2O-5.0-20 gives a short circuit current density of 6.5 mA/cm^2, an open-circuit voltage of 0.57 V, and a fill factor of 55.4%, yielding a power conversion efficiency of 2.03%. When the pH was changed to ~5.4, the corresponding values are J_{SC} = 11.3 mA/cm^2, V_{OC} = 0.56 V, FF = 49.6%, and η = 3.13%. The increased pH leads to an increase of 73.9% in J_{SC} and an enhancement of 54.2% in η. While maintaining the pH constant and extending the electrodeposition time to 60 min, the values turn to J_{SC} = 10.8 mA/cm^2, V_{OC} = 0.56 V, FF = 43.5%, and η = 2.61%. It is clear that, while the V_{OC} is same, there is a decrease in J_{SC} and η for the cell prepared for longer time. Compared with Cu_2O-5.8-20, the R_S values of Cu/Cu_2O solar cells are greatly reduced, and the cell based on Cu/Cu_2O-5.4-20 gives the smallest value, which is 221 Ω. When the content of Cu metal became higher, the values of R_S increased instead. Though the solar cells based on electrodeposited Cu_2O often give a low performance, the performance of our devices are better than many reported solar cells based on Cu_2O.

Table 1. Characteristics of solar cells based on four different photoanodes.

Photoanodes	J_{SC} [mA cm^{-2}]	V_{OC} [V]	FF [%]	η [%]	R_S [Ω]	R_{SH} [Ω]
Cu_2O-5.8-20	0.5	0.10	25.3	0.013	1695	1547
Cu/Cu_2O-5.0-20	6.5	0.57	55.4	2.03	291	2632
Cu/Cu_2O-5.4-20	11.3	0.56	49.6	3.13	221	1715
Cu/Cu_2O-5.4-60	10.8	0.56	43.5	2.61	319	1310

In dark condition, the electrodes passed almost only anodic current under forward bias, and no obvious battery effect can be observed in the cells. Considering the performances of the various cells, we can see that by implementing additional Cu metal, the short circuit current density and overall light conversion efficiency could be significantly increased. However, when the content of Cu metal is too much, there is a decrease in the performance. The efficiency change caused by Cu metal can be explained by considering a combination of several effects. First, Cu metal decreased the resistances of the films dramatically, which could contribute to the charge transfer; Second, Cu metal might help to trap the light. However, too much Cu is an obstacle to the effective use of light. Cu metal is intrinsically unstable in the polyiodide electrolyte, fast reactions occur when they meet.

To gain further insight on the inner work process of solar cells, electrochemical impedance spectrum (EIS) was measured under light illumination. The impedance spectra were also strongly affected by the amount of Cu. The inset image in **Figure 6**a represents that in the case of Cu_2O-5.8-20, the Nyquist plots consist of a low-frequency arc, and the global resistance is very large because of the high resistivity of the Cu_2O, which shows consistence with the big value of R_S. This

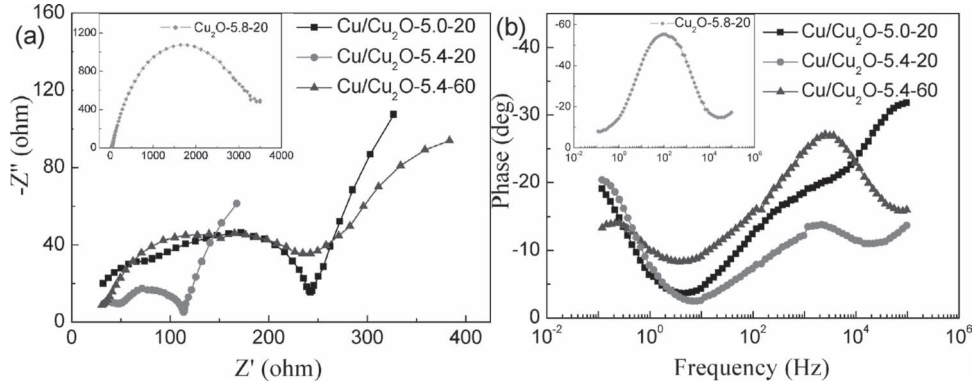

Figure 6. Electrochemical impedance spectra of cells with different electrodes. (a) Nyquist plots, (b) Bode plots. The inside images are the corresponding characteristics of Cu_2O-5.8-20.

parameter may suggest the poor performance. The resistivity is significantly reduced with the introduction of Cu. As shown in Figure 6a, the Nyquist plots of cells based on Cu/Cu_2O consist of one arc and one line. The arcs are compressed, which results from the inhomogeneities of the electrical properties of the measured interface.[33] According to the EIS model reported in other literatures,[34–37] the shape and size of the depressed semicircle was linked to the photo-injected electron transport in the Cu/Cu_2O film or the back reaction at the Cu/Cu_2O/electrolyte interface (the electrons in Cu/Cu_2O back to the electrolyte); the line in the low frequency range is associated with the Warburg diffusion of the ions in the electrolyte. The linear behavior indicates that there is slow ionic diffusion in the electrolyte system. Compared with that of Cu_2O-5.8-20, the semicircles of Cu/Cu_2O are reduced in number; this indicates that the charge transport resistance is reduced by introducing Cu. This may be due to the better charge transfer property between Cu/Cu_2O and electrolyte owing to the randomly distributed Cu/Cu_2O spheres on top of the Cu_2O thin films as shown in Figure 2.[21] The low transfer resistance could be an important factor for the improvement of the performance of cells. Among the cells based on Cu/Cu_2O photoanodes, Cu/Cu_2O-5.4-20 has the smallest semicircle, suggesting that the sample has the best transfer ability. When the Cu content reincreases, the semicircles increase in magnitude and the cell global resistance increased again. This may be caused by the increased charge recombination.

Figure 6b exhibits the Bode plots of the cells with different electrodes. It can be seen that the high frequency peak of Cu/Cu_2O-5.4-20 is shifted to lower frequency compared with that of Cu/Cu_2O-5.0-20 and Cu/Cu_2O-5.4-60. This result confirms that the solar cells based on Cu/Cu_2O-5.4-20 have the least charge recombination.[38]

Based on the above experimental facts, the electrode structure and a possible charge transfer mechanism in the Cu/Cu_2O contacts are proposed as shown in **Figure 7**. The Fermi level of Cu_2O is located at a more negative level than that of Cu metal. When Cu_2O is in contact with Cu, the band structure of Cu_2O (both the valence band (VB) and the conduction band (CB)) is bent as shown in Figure 7(b). Under irradiation, excitation of electrons from the VB to CB in the Cu_2O takes place, leaving holes in the VB. The electron and the hole form an excited electron-hole pair, which is usually short-lived and recombines if there is no driving force to separate them.[39] However, when the band structure is bent as in Figure 7(b), the photoexcited electrons from Cu_2O are likely to move to the metal core, while holes migrate to the surface, thus the hole and the electron can be separated.[40] In a typical p–n junction, electrons or holes excited by photoexcitation are accumulated firstly and then

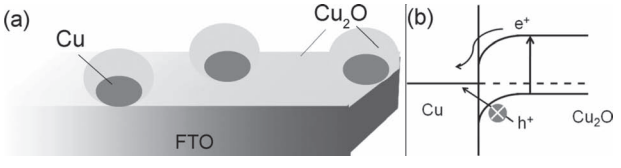

Figure 7. A schematic illustration of the structure and the possible charge transfer mechanism in the Cu/Cu_2O contacts.

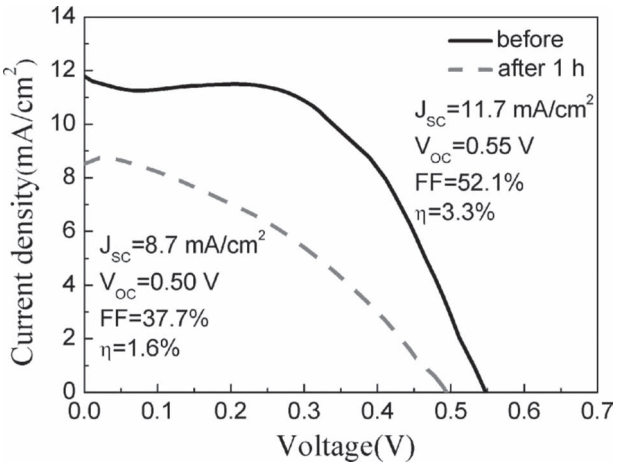

Figure 8. Photocurrent–voltage characteristics of a cell before and after 1 h of exposure to full sun condition at short circuit.

create electric currents. In contrast, the photoexcited electrons from Cu_2O are likely to move to the Cu core, and drift directly instead of accumulating. That is, the schottky junction can not only assist the charge separation, but also can transfer the dissociated electrons quickly. In this case, the Cu acts as a directional conductive pathway, which allows the charge transportation quickly and effectively, thus the adverse reactions (recombination and back reaction) are suppressed and the efficiency of the cells are improved. After such dissociation and migration of holes and electrons, the holes can oxidize the donor in the liquid electrolyte, and the electrons are transported to the FTO and then to the cathode reducing electron acceptors there.

The stability test was run at short circuit for 1 h under full sun condition. As shown in **Figure 8**, after 1 h, the J_{SC} decreased from 11.7 mA/cm^2 to 8.7 mA/cm^2, the values of V_{OC} and FF were both reduced, yielding a power conversion efficiency of 1.6%. This may be due to the corrosion of the redox electrolyte. Studies to improve long-term stability are under way. Samples using other electrolytes such as decamethylcobaltocene$^{+/0}$ redox couple are supposed to be more stabilizing. It is necessary to mention that the samples are sensitive to the pH and temperature and exhibit individual differences. In some samples, the particles on the spheres cannot protect Cu well, so there are redox peaks when being tested.

Besides, the Cu/Cu_2O can be electrodeposited on ITO/PEN substrates to form flexible solar cells. With the electrode of Cu/Cu_2O obtained by electrodepositing at pH 5.4 for 20 min (labeled as PEN-5.4-20), the cell achieves an efficiency of 1.44% (as shown in **Figure 9**). Other parameters are J_{SC} = 3.9 mA/cm^2, V_{OC} = 0.57 V, FF = 64.8%, and R_S = 304 Ω, R_{SH} = 4275 Ω. In the case of PEN-5.8-20, which was prepared by electrodepositing at pH 5.8 for 20 min, the corresponding values are J_{SC} = 0.5 mA/cm^2, V_{OC} = 0.13 V, FF = 21.6%, η = 0.015% and R_S = 3531 Ω, R_{SH} = 1585 Ω. We can see that the values of pH have similar influences on the performances of flexible cells.

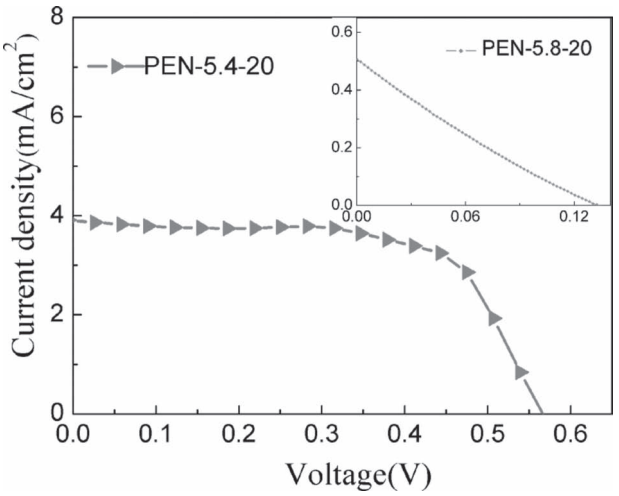

Figure 9. Photocurrent–voltage characteristics of plastic cells with different electrodes. The orange curve is of PEN-5.4-20 and the pink curve in the inside image is of PEN-5.8-20, respectively.

3. Conclusion

In summary, we have successfully prepared semiconductor-liquid junction solar cells based on Cu/Cu_2O and pure Cu_2O. The photoelectrodes were synthesized by a simple electrodepositing process at low temperature, which is suitable for industrial production. The values of the electrolyte pH have great influence on the morphology and the compositions of the obtained films, and thus affect the performance of the cells. It is shown that the introducing of Cu metal can greatly improve the performances of Cu_2O solar cells. The best device based on Cu/Cu_2O and I^-/I_3^- electrolyte reached an open-circuit voltage of 0.56 V, a short-circuit current density of 11.3 mA/cm^2, a fill factor of 49.6%, and a conversion efficiency of 3.13% under simulated AM1.5G illumination. In contrast, the performance of the solar cells based on pure Cu_2O is very poor, as low as 0.013%. In addition, the films are also electrodeposited on ITO-PEN plastics to form flexible solar cells. The values of pH have similar influences on the performances of the flexible cells. The flexible cells based on Cu/Cu_2O films gave a power conversion efficiency of 1.44%.

4. Experimental Section

Preparation of Cu/Cu_2O and Cu_2O photoanodes: Electrodepositions of Cu/Cu_2O were performed using a standard three-electrode cell where FTO glasses, saturated calomel electrode and platinum were used as the working, reference and counter electrode, respectively. The electrolyte was composed of cupric acetate (0.02 M) and sodium acetate (0.1 M), to which sodium hydroxide solution and acetic acid were added to adjust the pH. The samples were deposited potentiostatically at –245 mV and the temperature was maintained at 60 °C. After each deposition, the obtained film was rinsed with ethanol and then dried in an electric oven at 60 °C.

For comparison purposes, pure Cu_2O films were deposited from aqueous solutions with different pH. Moreover, effects of the pH and the deposition time were also studied. The as prepared samples were denoted as Cu/Cu_2O-x-y or Cu_2O-x-y, where x (5.0, 5.4, or 5.8), y (20 or 60) referred to the corresponding pH and deposition time (min), respectively. We also prepared flexible solar cells by substituting the FTO glasses with ITO-PEN plastic substrates.

Fabrication of solar cell: The solar cells were composed of a photoanode, a platinum-sputtered FTO counter electrode, and liquid electrolyte. The photoanodes were Cu/Cu_2O films or pure Cu_2O films electrodeposited on FTO glasses or ITO-PEN plastics. The two electrodes were separated by a spacer. The internal space of the cells was filled with the electrolyte which contains LiI (0.5 M), I_2 (0.05 M) and tert-butylpyridine (0.5 M) in acetonitrile.

Characterization of samples: Compositions of the as-prepared samples were investigated by X-ray diffraction (XRD, D/max 2550V, Rigaku Tokyo, Japan) and energy dispersive spectrometer (EDS), respectively. The morphology was characterized with field emission scanning electron microscopy (FESEM, JSM-6700F, JEOL Tokyo, Japan). The total transmission and total reflection of the samples were recorded with a lambda-950 UV-Vis spectrophotometer (Perkin Elmer, Waltham, MA). Current density voltage (*J–V*) characteristics of the solar cells were measured on an electrochemical workstation (Model CHI 660C, CH) under an AM 1.5 illumination (100 mW/cm^2, Model YSS-80A, Yamashita). The light source was Xe lamp equipped with an AM1.5G filter. Prior to measurements, an aperture mask was employed for the calibration of the cell area, which was 0.12 cm^2. Dark current voltage characteristics were performed on CHI 660D electrochemical workstation. The incident light intensity was 100 mW/cm^2 calibrated with a standard Si solar cell. Electrochemical impedance spectroscopic (EIS) curves of the cells were carried out in the frequency range from 0.1 Hz to 100 kHz under open-circuit conditions. In the stability test, the *J–V* curves were recorded by a Keithley Series 2400 System Source Meter Instrument. The irradiation source is a solar simulator (Newport) giving AM 1.5 G illumination on the surface of the solar cells.

Supporting Information

Supporting Information is available from the Wiley Online Library or from the author.

Acknowledgements

This work was supported by the National Natural Science Foundation of China (Grant No. 50972157, 51072215). We thank help from Mr. Wei Wu on the components characterization by scanning electron microscopy and energy dispersive spectrometer. We appreciate the fruitful discussion with Prof. Wenqing Zhang and Prof. Fuqiang Huang.

Received: February 7, 2012
Revised: March 23, 2012
Published online: June 4, 2012

[1] T. Mahalingam, J. S. P. Chitra, J. P. Chu, H. Moon, H. J. Kwon, Y. D. Kim, *J. Mater. Sci.-Mater. Electron.* **2006**, *17*, 519.
[2] Y. W. Tang, Z. G. Chen, Z. J. Jia, L. S. Zhang, J. L. Li, *Mater. Lett.* **2005**, *59*, 434.
[3] C. A. N. Fernando, N. T. R. N. Kumara, T. N. Gamage, *Semicond. Sci. Technol.* **2010**, 25.
[4] Y. Hou, X. Y. Li, Q. D. Zhao, X. Quan, G. H. Chen, *Appl. Phys. Lett.* **2009**, 95.
[5] T. Mahalingam, J. S. P. Chitra, G. Ravi, J. P. Chu, P. J. Sebastian, *Surf. Coat. Technol.* **2003**, *168*, 111.
[6] X. Y. Liu, R. Z. Hu, S. L. Xiong, Y. K. Liu, L. L. Chai, K. Y. Bao, Y. T. Qian, *Mater. Chem. Phys.* **2009**, *114*, 213.
[7] J. B. Cui, U. J. Gibson, *J. Phys. Chem. C* **2010**, *114*, 6408.
[8] W. Shockley, H. J. Queisser, *J. Appl. Phys.* **1961**, *32*, 510.
[9] Z. K. Zheng, B. B. Huang, Z. Y. Wang, M. Guo, X. Y. Qin, X. Y. Zhang, P. Wang, Y. Dai, *J. Phys. Chem. C.* **2009**, *113*, 14448.

[10] L. Huang, S. Zhang, F. Peng, H. Wang, H. Yu, J. Yang, S. Zhang, H. Zhao, *Scripta Mater.* **2010**, *63*, 159.
[11] Y. Hou, X. Y. Li, X. J. Zou, X. Quan, G. C. Chen, *Environ. Sci. Technol.* **2009**, *43*, 858.
[12] L. Huang, F. Peng, H. J. Wang, H. Yu, Z. Li, *Catal. Commun.* **2009**, *10*, 1839.
[13] K. Lalitha, G. Sadanandam, V. D. Kumari, M. Subrahmanyam, B. Sreedhar, N. Y. Hebalkar, *J. Phys. Chem. C* **2010**, *114*, 22181.
[14] C. A. N. Fernando, *Sol. Energy Mater. Sol. Cells* **1993**, *28*, 375.
[15] G. K. Paul, R. Ghosh, S. K. Bera, S. Bandyopadhyay, T. Sakurai, K. Akimoto, *Chem. Phys. Lett.* **2008**, *463*, 117.
[16] A. Mittiga, S. S. Jeong, E. Salza, A. Masci, S. Passerini, *Electrochim. Acta* **2008**, *53*, 2226.
[17] K. P. Hewaparakrama, C. Jayewardena, D. L. A. Wijewardena, H. Guruge, *Sol. Energy Mater. Sol. Cells* **1998**, *56*, 29.
[18] A. Mittiga, E. Salza, F. Sarto, M. Tucci, R. Vasanthi, *Appl Phys Lett* **2006**, 88.
[19] K. P. Musselman, A. Wisnet, D. C. Iza, H. C. Hesse, C. Scheu, J. L. MacManus-Driscoll, L. Schmidt-Mende, *Adv. Mater.* **2010**, *22*, E 254.
[20] I. C. Chen, T. J. Hsueh, C. L. Hsu, S. J. Changa, P. W. Guo, J. H. Hsieh, *Scripta Mater.* **2007**, *57*, 53.
[21] R. P. Wijesundera, M. Hidaka, K. Koga, M. Sakai, W. Siripala, *Thin Solid Films* **2006**, *500*, 241.
[22] J. A. Assimos, D. Trivich, *J. Appl. Phys.* **1973**, *44*, 1687.
[23] R. N. Briskman, *Sol. Energy Mater. Sol. Cells* **1992**, *27*, 361.
[24] G. Hodes, *J. Phys. Chem. C* **2008**, *112*, 17778.
[25] R. Jose, V. Thavasi, S. Ramakrishna, *J. Am. Ceram. Soc.* **2009**, *92*, 289.
[26] L. M. Goncalves, V. D. Bermudez, H. A. Ribeiro, A. M. Mendes, *Energy Environ. Sci.* **2008**, *1*, 655.
[27] C. X. Xiang, G. M. Kimball, R. L. Grimm, B. S. Brunschwig, H. A. Atwater, N. S. Lewis, *Energy Environ. Sci.* **2011**, *4*, 1311.
[28] Y. Tachibana, R. Muramoto, H. Matsumoto, S. Kuwabata, *Res. Chem. Intermed.* **2006**, *32*, 575.
[29] K. S. Choi, C. M. McShane, *J. Am. Chem. Soc.* **2009**, *131*, 2561.
[30] R. Inguanta, S. Piazza, C. Sunseri, *Electrochim. Acta* **2008**, *53*, 6504.
[31] H. S. Jang, S. J. Kim, K. S. Choi, *Small* **2010**, *6*, 2183.
[32] B. D. Yuhas, P. D. Yang, *J. Am. Chem. Soc.* **2009**, *131*, 3756.
[33] K. P. Musselman, A. Marin, A. Wisnet, C. Scheu, J. L. MacManus-Driscoll, L. Schmidt-Mende, *Adv. Funct. Mater.* **2011**, *21*, 573.
[34] L. X. Li, X. C. Tang, H. T. Liu, Y. Qu, Z. G. Lu, *Electrochim. Acta* **2010**, *56*, 995.
[35] Y. R. Wang, Y. F. Yang, Y. B. Yang, H. X. Shao, *Solid State Commun.* **2010**, *150*, 81.
[36] L. Wang, H. B. Wang, Z. H. Liu, C. Xiao, S. M. Dong, P. X. Han, Z. Y. Zhang, X. Y. Zhang, C. F. Bi, G. L. Cui, *Solid State Ionics* **2010**, *181*, 1685.
[37] Y. K. Zhou, J. Wang, Y. Y. Hu, R. O'Hayre, Z. P. Shao, *Chem. Commun.* **2010**, *46*, 7151.
[38] L. P. Heng, X. Y. Wang, N. L. Yang, J. Zhai, M. X. Wan, L. Jiang, *Adv. Funct. Mater.* **2010**, *20*, 266.
[39] M. Kaneko, H. Ueno, J. Nemoto, *Beilstein J. Nanotechnol.* **2011**, *2*, 127.
[40] C. H. Kuo, Y. C. Yang, S. Gwo, M. H. Huang, *J. Am. Chem. Soc.* **2011**, *133*, 1052.